Electronic Supplementary Information (ESI) for:

Versatile Functionalization of De-Fluorinated FMOF-1 Towards Enhanced Carbon Capture and Separation: A Predictive Molecular Simulation Study

Rashida Yasmeen,[1] Sheikh M. S. Islam,[2] Jincheng Du,[1,*] and Mohammad A. Omary[2,*]

[1]*Department of Materials Science & Engineering, University of North Texas, 1155 Union Circle, Denton, Texas-76203, United States*

[2]*Department of Chemistry, University of North Texas, 1155 Union Circle, Denton, Texas-76203, United States*

*Corresponding Authors. Jincheng Du, Email: Jincheng.Du@unt.edu
Mohammad A. Omary, Email: Omary@unt.edu

Contents

S1. Geometry optimization of X-functionalized MOFs

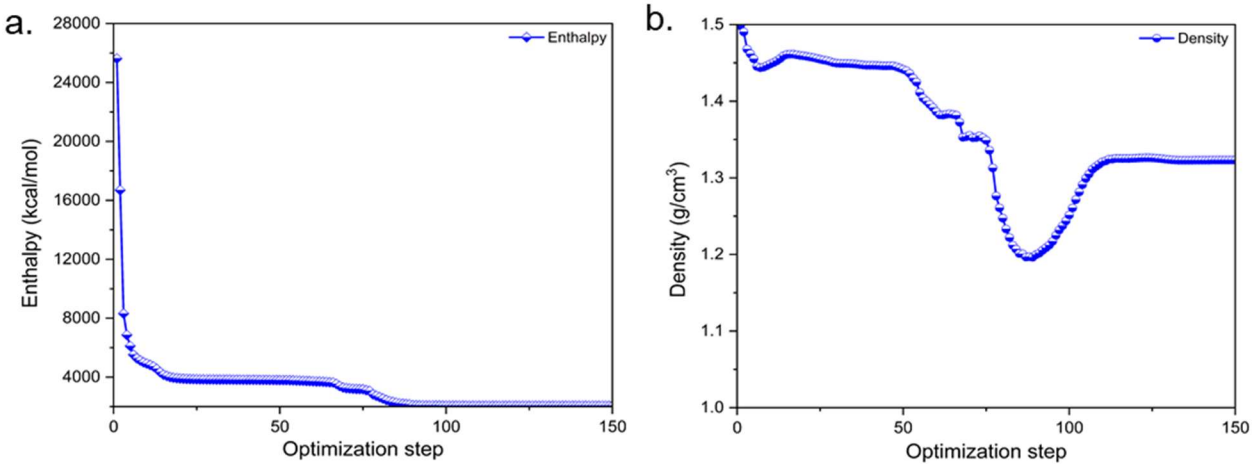

Figure S1. Forcite geometry optimization: (a) energy and (b) density of FMOF-1-OCH_3.

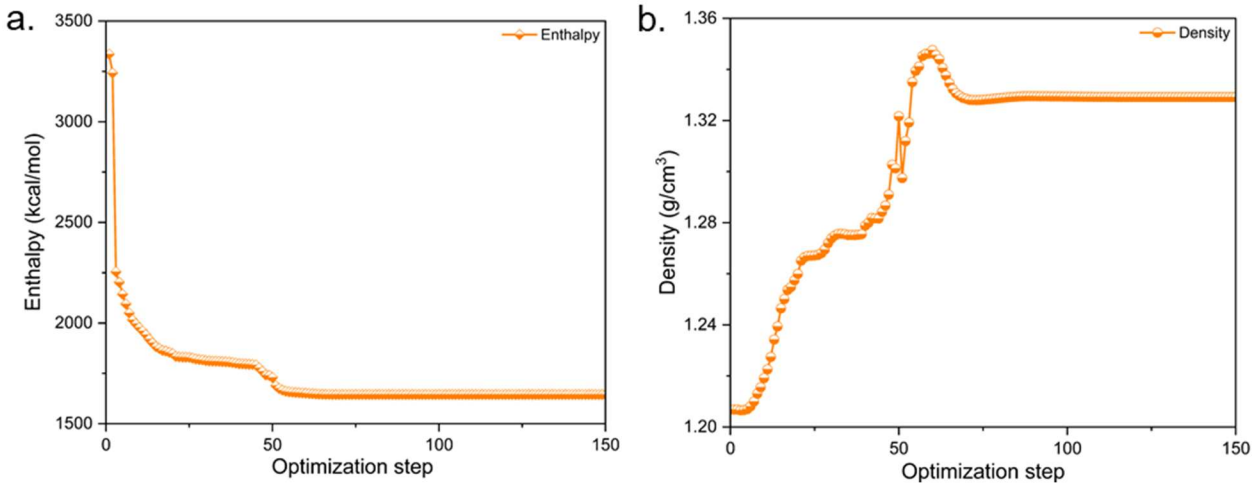

Figure S2. Forcite geometry optimization: (a) energy and (b) density of FMOF-1-CN.

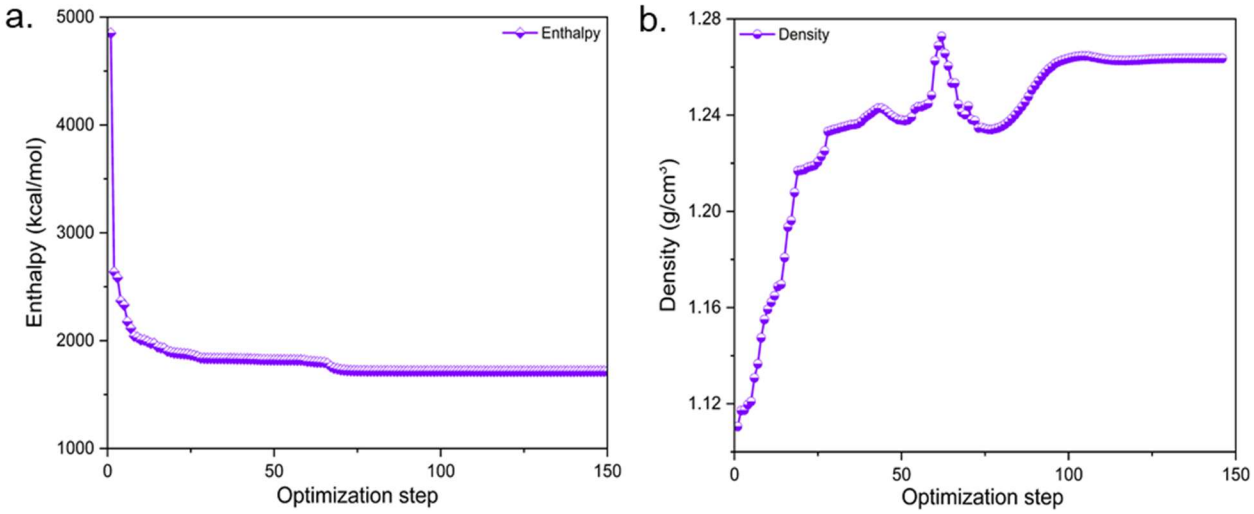

Figure S3. Forcite geometry optimization: (a) energy and (b) density of FMOF-1-OH.

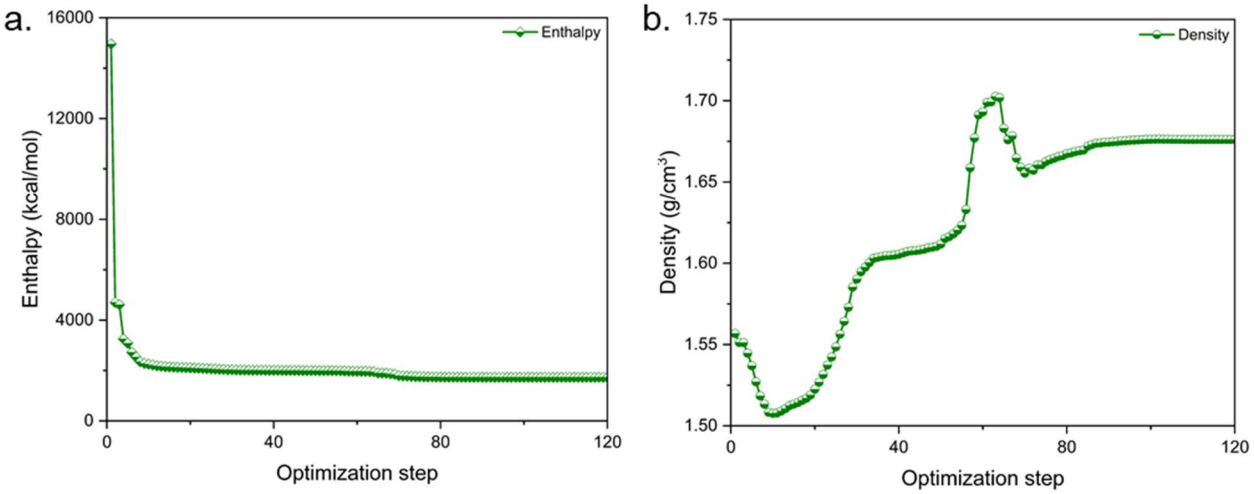

Figure S4. Forcite geometry optimization: (a) energy and (b) density of FMOF-1-COOH.

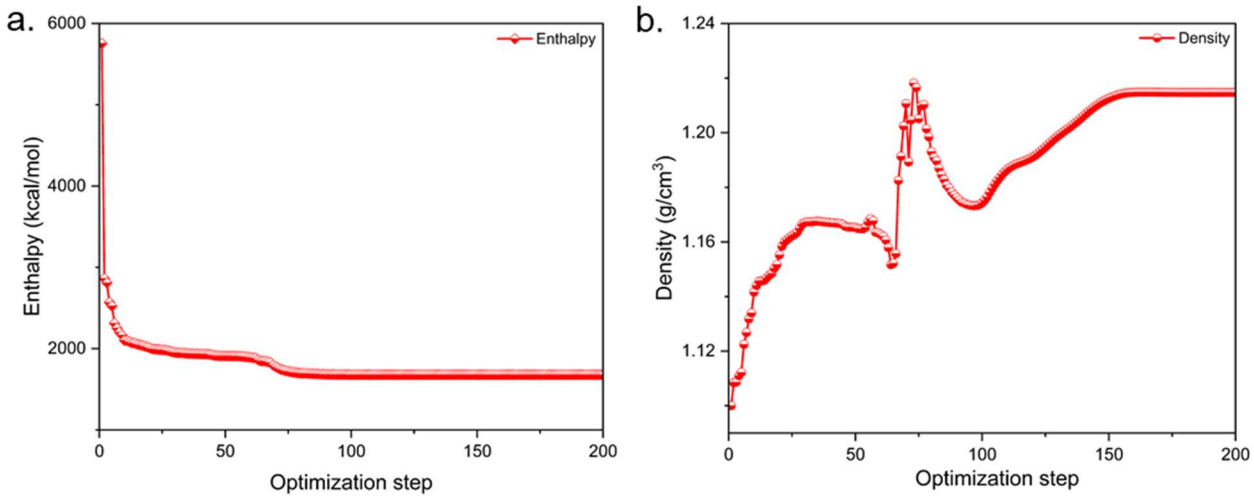

Figure S5. Forcite geometry optimization: (a) energy and (b) density of FMOF-1-NH_2.

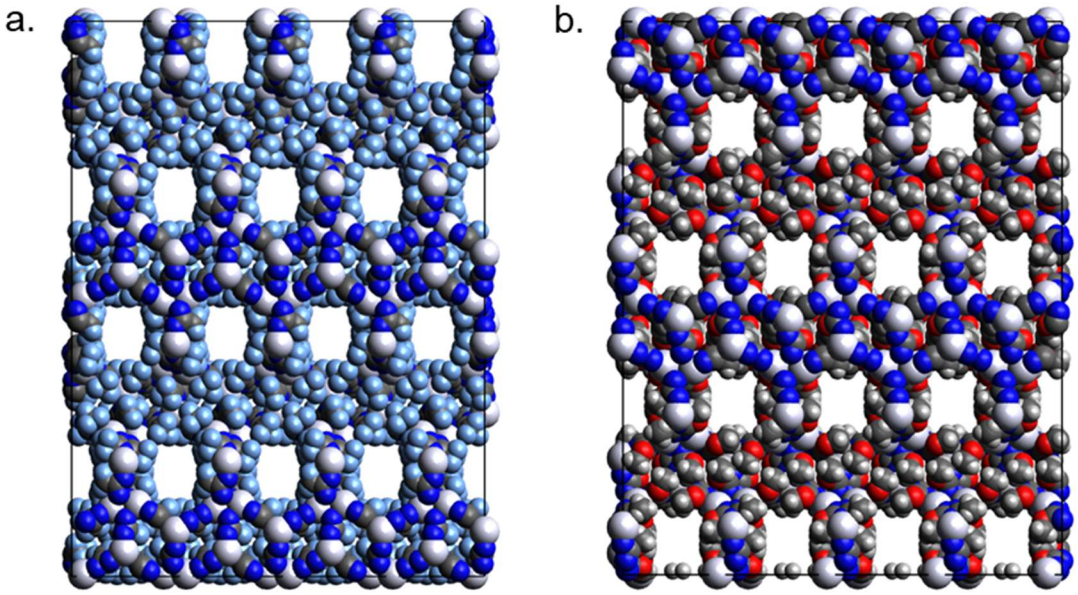

Figure S6. Crystal structures of (a) FMOF-1 and (b) FMOF-1-OCH_3.

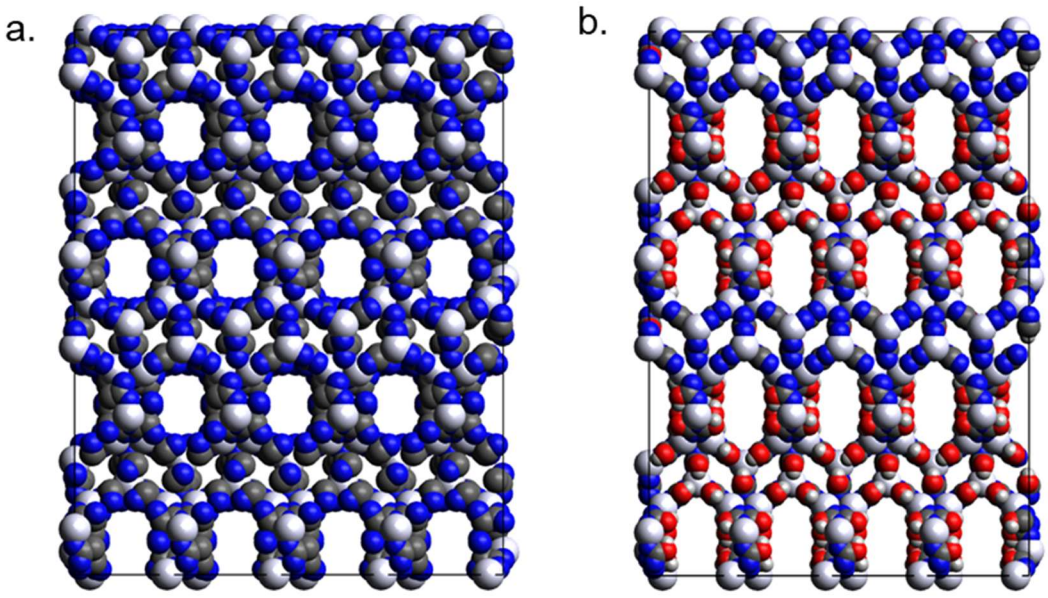

Figure S7. Crystal structures of (a) FMOF-1-CN and (b) FMOF-1-OH.

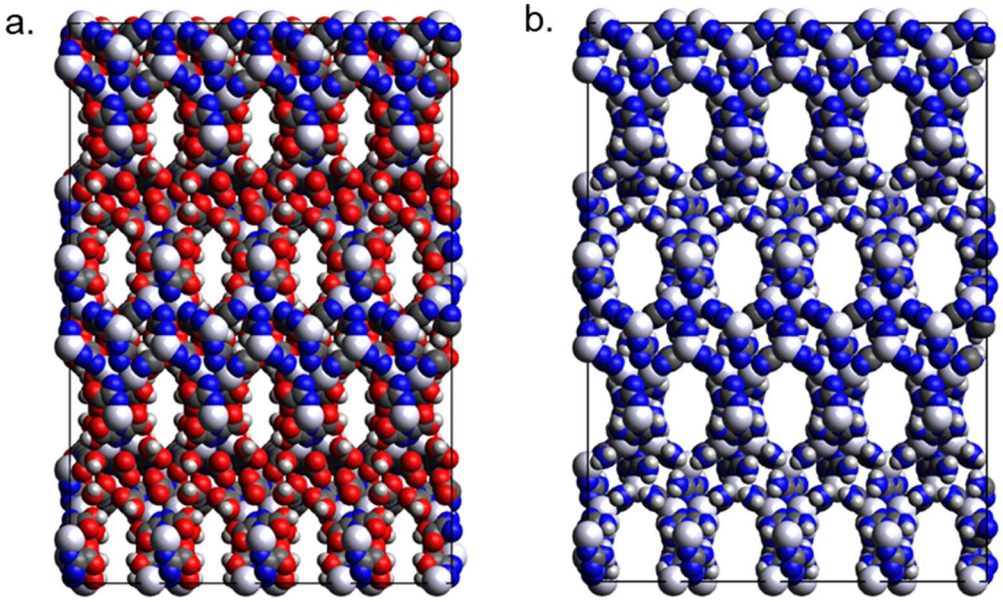

Figure S8. Crystal structures of (a) FMOF-1-COOH and (b) FMOF-1-NH_2.

S2. Lennard-Jones (L-J) parameters and partial charges

Table S1. Lennard-Jones parameters of the frameworks.

Atom type	σ (Å)	ε/k_B (K)	Force field
N	3.26	34.60	UFF[1]
C	3.43	52.40	UFF[1]
F	3.09	25.20	UFF[1]
H	2.57	22.14	UFF[1]
Ag	2.81	18.12	UFF[1]

Table S2. Atomic partial charges (e) for FMOF-1.[2]

Atom	Ag_1	Ag_2	N_1	N_2	C_1	C_2	F
Charge	0.350	0.390	-0.347	-0.384	0.345	0.51	-0.17

**C_2 and F corresponds to -CF_3 functional group.*

Table S3. Atomic partial charges (e) for FMOF-1-OCH_3.

Atom	Ag_1	Ag_2	N_1	N_2	C_1	C_2	O	H
Charge	0.308	0.372	-0.347	-0.384	0.548	-0.390	-0.150	0.118

**C_2, O and H corresponds to -OCH_3 functional group.*

Table S4. Atomic partial charges (e) for FMOF-1-CN.

Atom	Ag_1	Ag_2	N_1	N_2	N_3	C_1	C_2
Charge	0.350	0.390	-0.347	-0.384	-0.268	0.345	0.268

**N_3 and C_2 corresponds to -CN functional group.*

Table S5. Atomic partial charges (e) for FMOF-1-OH.

Atom	Ag_1	Ag_2	N_1	N_2	C_1	O	H
Charge	0.350	0.390	-0.347	-0.384	0.345	-0.562	0.562

**O and H corresponds to -OH functional group.*

Table S6. Atomic partial charges (e) for FMOF-1-COOH.

Atom	Ag_1	Ag_2	N_1	N_2	C_1	C_2	O_1	O_2	H
Charge	0.351	0.391	-0.174	-0.211	0.068	0.556	-0.423	-0.529	0.410

**C_2, O_1, O_2 and H corresponds to -COOH functional group.*

Table S7. Atomic partial charges (e) for FMOF-1-NH_2.

Atom	Ag_1	Ag_2	N_1	N_2	N_3	C_1	H
Charge	0.318	0.358	-0.386	-0.420	-1.112	-0.505	0.513

**N_3 and H corresponds to -NH_2 functional group.*

Table S8. Lennard-Jones parameters and partial charges of the adsorbates used in this work.

Adsorbate	Atom type	σ (Å)	ε/k_B (K)	q (e)	Force field
Carbon dioxide	O_CO_2	3.05	79.0	-0.350	TraPPE[3]
	C_CO_2	2.80	27.0	0.700	TraPPE[3]
Methane	CH_4	3.73	148.0	0.000	TraPPE[4]
Nitrogen	N_N_2	3.31	36.0	-0.482	TraPPE[3]
	N_com	0.0	0.0	0.964	TraPPE[3]

S3. Excess and absolute adsorption

Excess adsorption amount is obtained from experimental measurements, whereas absolute uptake is calculated from simulations. The excess (n^{ex}) and absolute (n^{abs}) uptake are related to each other as per the following equation,[5]

$$n^{ex} = n^{abs} - V^g \rho^g$$

Where V^g is the pore volume of the MOF and ρ^g is the molar density of the bulk gas phase. Generally, RASPA2 software calculate the absolute adsorption first.[6] During simulation we specify the pore volume of the MOF as void fraction (probed with helium), and ρ^g is calculated by the Peng-Robinson equation of state. After obtaining all the parameters, RASPA2 determine the excess adsorption amount using above equation.

S4. N_2 uptake comparison of this work with previously reported data

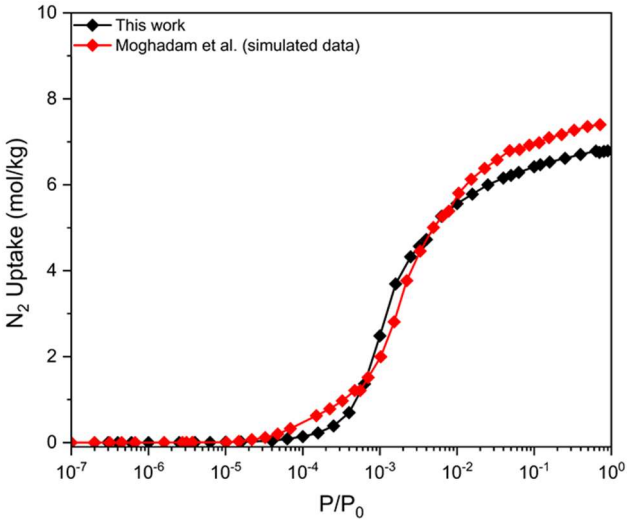

Figure S9. Comparison of N_2 uptake with previously reported data at 77 K in FMOF-1c.[2]

S5. N_2 uptake data at 77 K

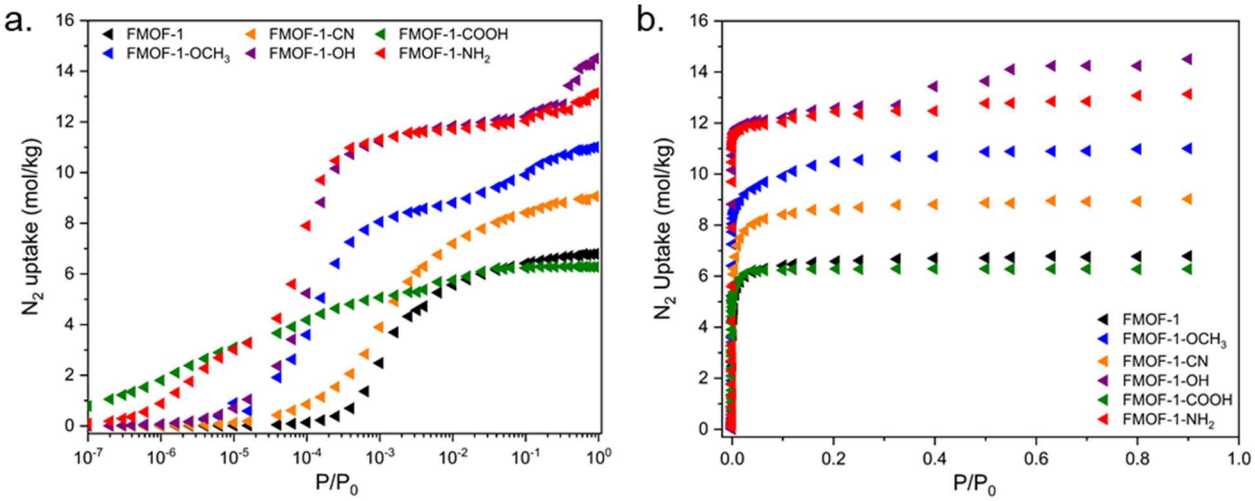

Figure S10. N_2 adsorption isotherm of MOFs at 77 K in (a) logarithmic and (b) normal scale.

S6. Energy parameters at 273 K

Table 9. Henry's constant, K_H at 273 K.

Structure	Henry's constant, K_H (mol/kg/Pa)		
	CO_2	CH_4	N_2
FMOF-1	3.34×10^{-6}	1.88×10^{-6}	6.92×10^{-7}
FMOF-1-OCH_3	7.78×10^{-6}	3.46×10^{-6}	1.11×10^{-6}
FMOF-1-CN	9.90×10^{-6}	2.04×10^{-6}	8.75×10^{-7}
FMOF-1-OH	1.09×10^{-4}	1.98×10^{-6}	1.13×10^{-6}
FMOF-1-COOH	3.19×10^{-4}	3.60×10^{-6}	1.65×10^{-6}
FMOF-1-NH_2	2.23×10^{-4}	3.20×10^{-6}	1.62×10^{-6}

Table 10. Isosteric heat of adsorption at infinite dilution, Q_{st0} at 273 K.

Structure	Isosteric heat of adsorption at infinite dilution, Q_{st0} (kJ/mol)		
	CO_2	CH_4	N_2
FMOF-1	-13.71	-11.54	-9.16
FMOF-1-OCH_3	-17.41	-13.20	-10.40
FMOF-1-CN	-18.10	-11.66	-9.60
FMOF-1-OH	-30.73	-10.50	-9.71
FMOF-1-COOH	-31.44	-15.50	-14.50
FMOF-1-NH_2	-31.82	-11.67	-10.85

S7. Adsorption isotherms and isosteric heats of adsorption at different temperatures

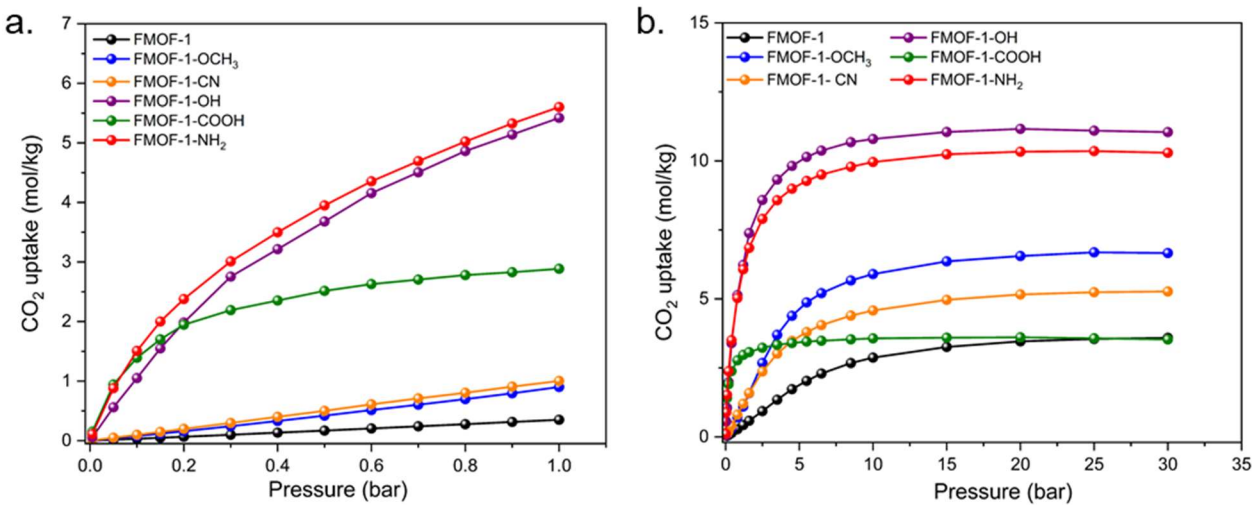

Figure S11. CO_2 adsorption isotherms at (a) low pressure and (b) high pressure regions of MOFs at 273 K.

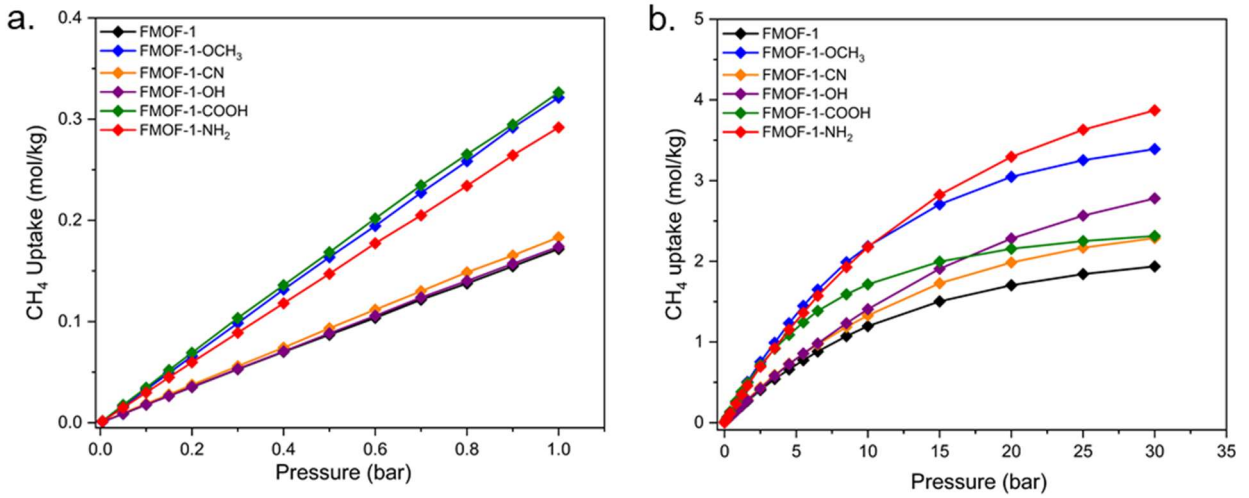

Figure S12. CH_4 adsorption isotherms at (a) low pressure and (b) high pressure regions of MOFs at 273 K.

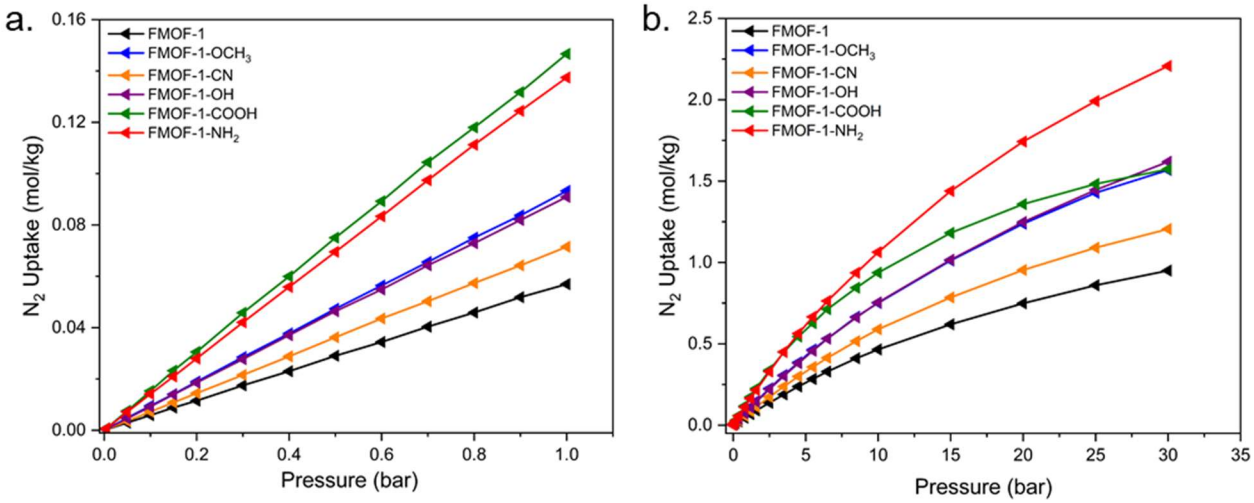

Figure S13. N_2 adsorption isotherms at (a) low pressure and (b) high pressure regions of MOFs at 273 K.

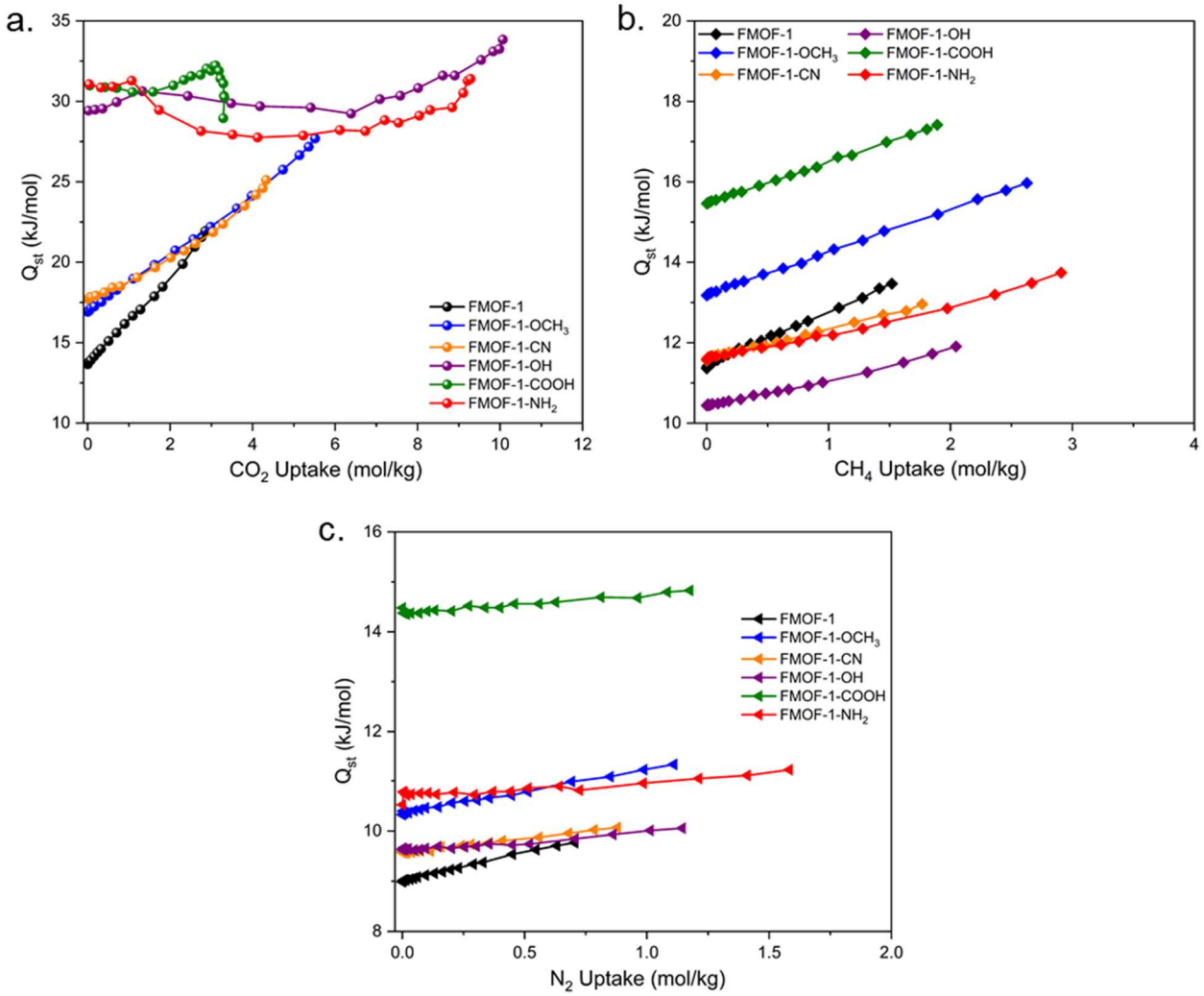

Figure S14. Isosteric heats of adsorption for (a) CO_2, (b) CH_4, and (c) N_2 at different loadings at 298 K.

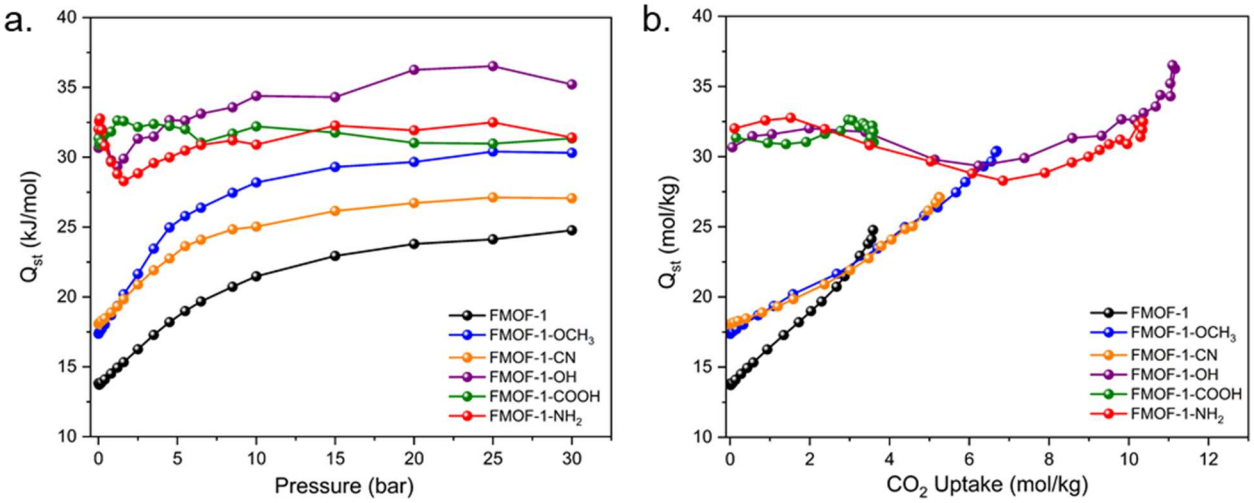

Figure S15. Isosteric heats of adsorption for CO_2 at different (a) pressure and (b) uptake at 273 K.

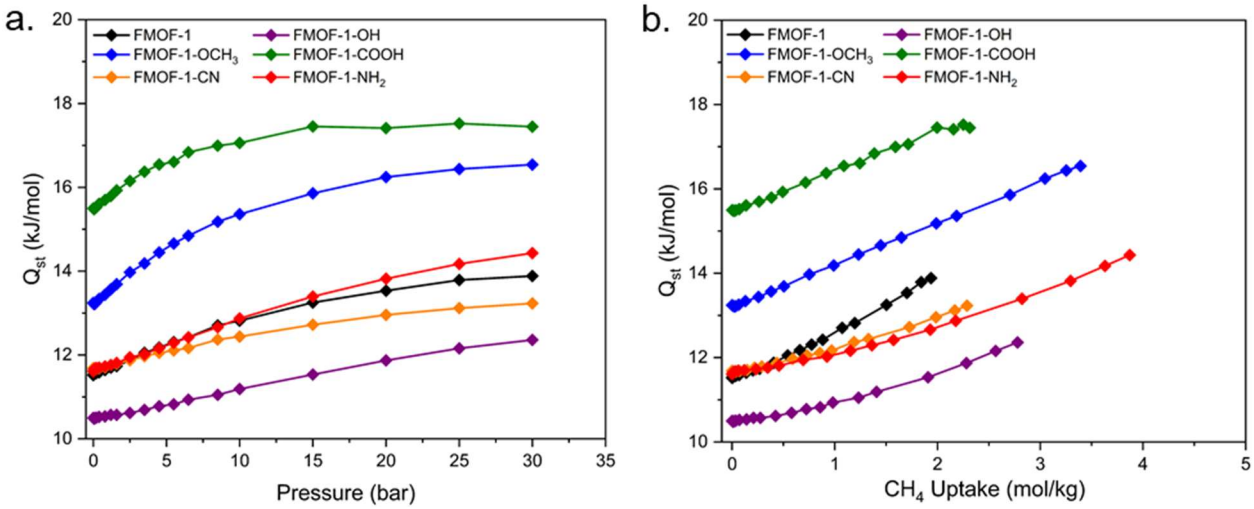

Figure S16. Isosteric heats of adsorption for CH_4 at different (a) pressure and (b) uptake at 273 K.

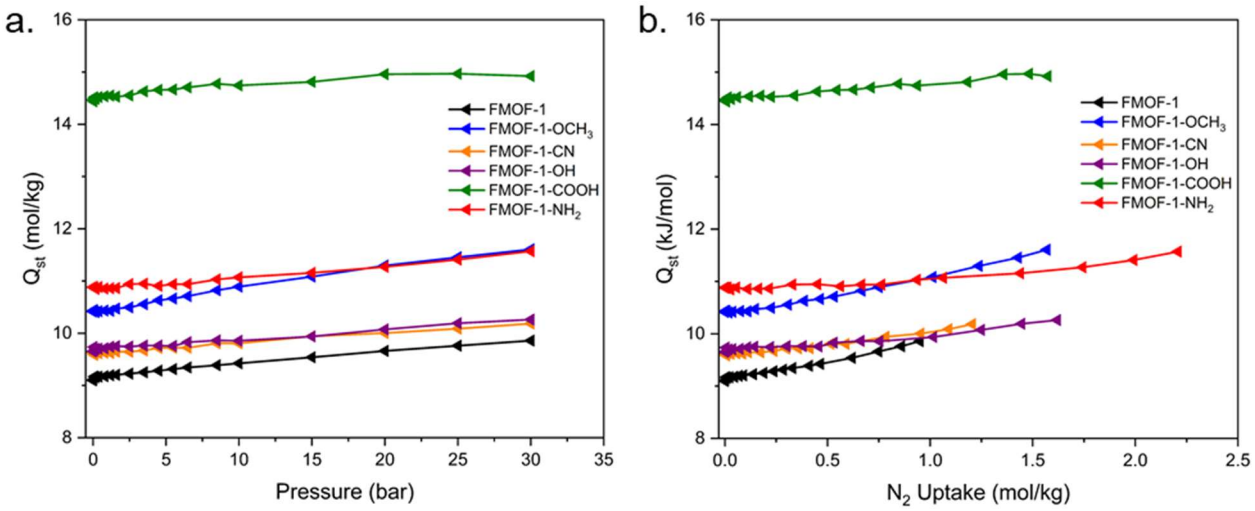

Figure S17. Isosteric heats of adsorption for N_2 at different (a) pressure and (b) uptake at 273 K.

S8. Effect of coulombic interaction on CH_4 and N_2 adsorption isotherms

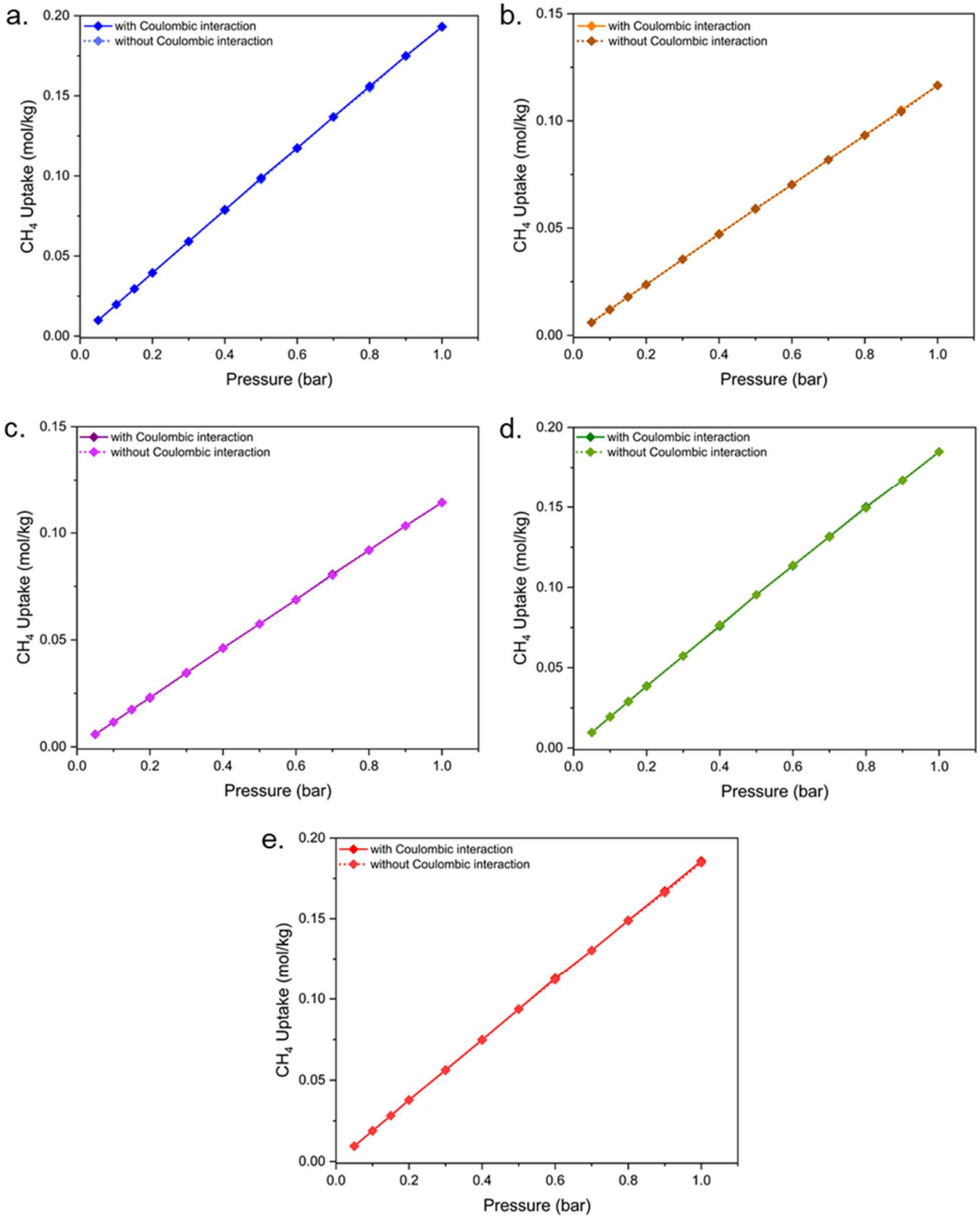

Figure S18. Comparison of CH_4 adsorption isotherms obtained by considering or neglecting electrostatic interactions in (a) FMOF-1-OCH_3, (b) FMOF-1-CN, (c) FMOF-1-OH, (d) FMOF-1-COOH, and (e) FMOF-1-NH_2 at 298 K.

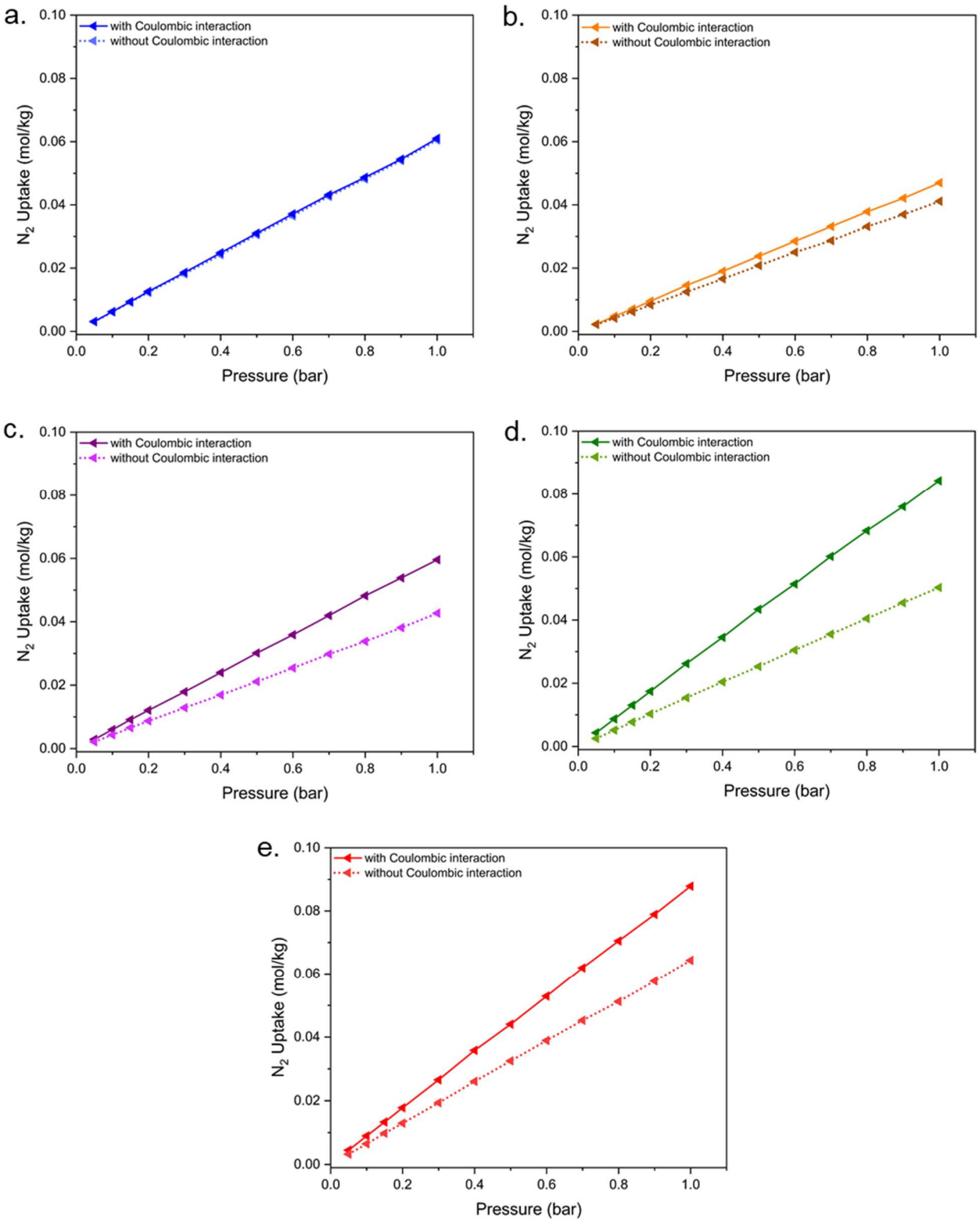

Figure S19. Comparison of N_2 adsorption isotherms obtained by considering or neglecting electrostatic interactions in (a) FMOF-1-OCH_3, (b) FMOF-1-CN, (c) FMOF-1-OH, (d) FMOF-1-COOH, and (e) FMOF-1-NH_2 at 298 K.

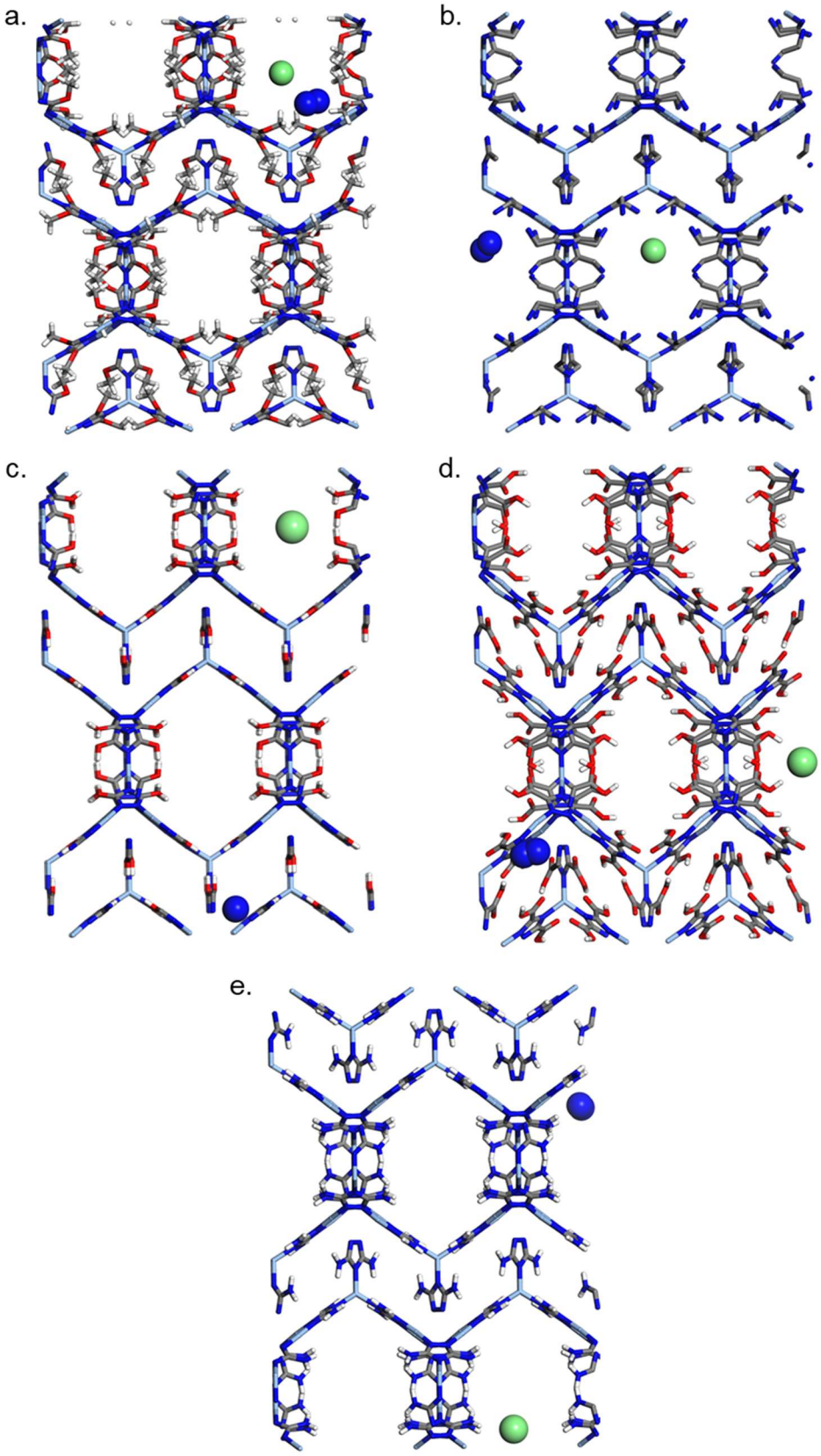

Figure S20. Adsorption sites of CH_4 (green sphere) and N_2 (blue sphere) in (a) -OCH_3, (b) -CN, (c) -OH, (d) -COOH, and (e) -NH_2 functionalized MOFs after Baker's minimization.

S9: CO_2/CH_4 and CO_2/N_2 selectivity

CO_2/CH_4 and CO_2/N_2 selectivity was calculated using the Ideal Adsorbed Solution Theory (IAST).[7] The selectivity of the strongly adsorbed component over the weakly adsorbed component was formulated as:

$$S_{1/2} = \frac{x_1/x_2}{y_1/y_2}$$

where, x_1 and x_2 are the absolute component uptakes of the adsorbed phase; and y_1 and y_2 are the mole fractions of the strongly and weakly adsorbed components in the bulk phases, respectively.

To attain the IAST selectivity, the simulated pure CO_2, CH_4, and N_2 adsorption isotherms at 298 K were fitted to the single-site Langmuir-Freundlich (L-F) model[8] according to the following equation:

$$n = \frac{a * b * P^c}{1 + b * P^c}$$

where, n is the adsorbed amount in mol/kg, P is the pressure in kPa and a, b, c are the fitting parameters.

We also estimated the selectivity by considering the Henry's constant ratio of the corresponding gases. The Henry's constants are correlated with the slope of CO_2, CH_4, and N_2 adsorption isotherms at very low loading (virtually zero-coverage). Although, the Henry's constant ratio provides only an approximate selectivity value of the material,[9] it is always good to compare the results obtained from different methods. The selectivity values derived from the corresponding Henry's constant ratios along with the selectivity values calculated by IAST method at 0.1 bar and 298 K for CO_2/CH_4 and CO_2/N_2 are shown in Figure S21(a) and S21(b), respectively.

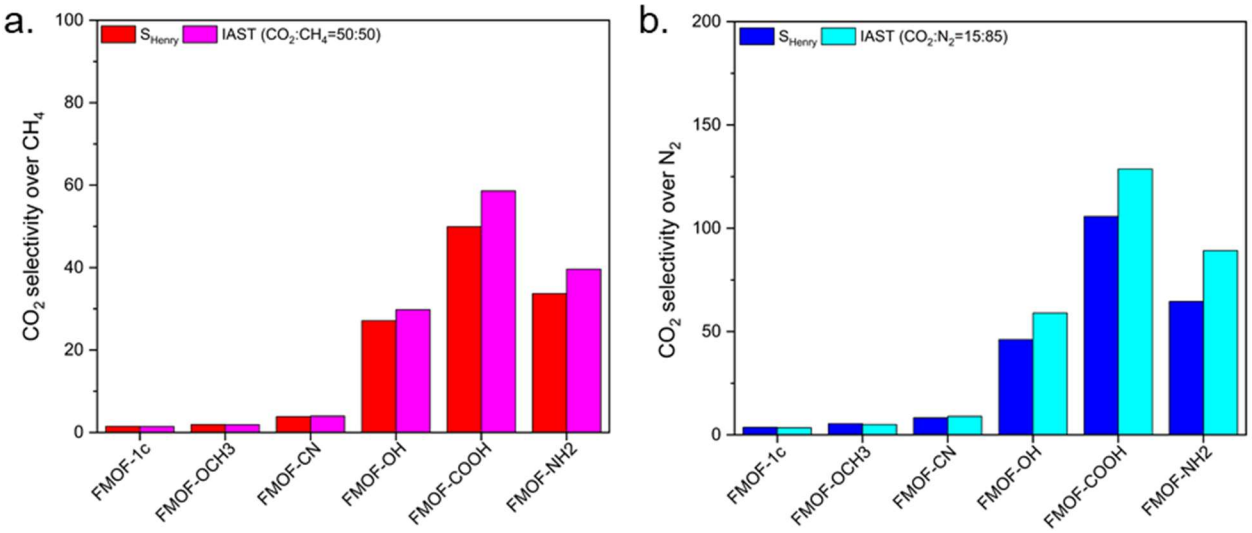

Figure S21. Adsorption selectivity for (a) CO_2/CH_4 and (b) CO_2/N_2 binary gas mixtures based on two different methods at 298 K.

Selectivity values obtained by the IAST method shows a certain degree of discrepancy compared to the values predicted from the Henry's constant ratios. For the -COOH functionalized MOF, we observe a sharp difference between the selectivity values obtained by the two methods for CO_2/CH_4 gas mixture. For the remaining MOF structures, we observe a higher selectivity values obtained by the IAST method than that of the Henry's constant ratios, but the difference is not sharp as the -COOH functionalized MOF. Like the CO_2/CH_4 gas mixture, we notice a similar trend for the CO_2/N_2 binary mixture for all the MOFs at 298 K.

References

1 A. K. Rappe, C. J. Casewit, K. S. Colwell, W. A. Goddard and W. M. Skiff, *J Am Chem Soc*, 1992, **114**, 10024–10035.

2 P. Z. Moghadam, J. F. Ivy, R. K. Arvapally, A. M. dos Santos, J. C. Pearson, L. Zhang, E. Tylianakis, P. Ghosh, I. W. H. Oswald, U. Kaipa, X. Wang, A. K. Wilson, R. Q. Snurr and M. A. Omary, *Chem Sci*, 2017, **8**, 3989–4000.

3 J. J. Potoff and J. I. Siepmann, *AIChE Journal*, 2001, **47**, 1676–1682.

4 M.G. Martin, J. I. Siepmann, *J Phys Chem B*, 1998, **102**, 2569–2577.

5 T. Düren and R. Q. Snurr, *J Phys Chem B*, 2004, **108**, 15703–15708.

6 D. Dubbeldam, S. Calero, D. E. Ellis and R. Q. Snurr, *Mol Simul*, 2016, **42**, 81–101.

7 A. L. Myers and J. M. Prausnitz, *AIChE Journal*, 1965, **11**, 121–127.

8 R. Sips, *J Chem Phys*, 1948, **16**, 490–495.

9 A. Torrisi, R. G. Bell and C. Mellot-Draznieks, *Cryst Growth Des*, 2010, **10**, 2839–2841.